Title: **Technical report for the DESIR High-Resolution Separator (DESIR-HRS)**

Authors: T. Kurtukian-Nieto[1], R. Baartman[2], T. Bataille[1], B. Blank[1], T. Chiron[1], C. Davids[3], F.Delalee[1], M. Duval[4], D. Lunney[5], F. Méot[6], L. Serani[1], M.-H. Stodel[4], F. Varenne[4], H. Weick[7]
([1] CENBG, [2] TRIUMF, [3] ANL, [4] GANIL, [5] CSNSM Orsay, [6] BNL, [7] GSI)

The DESIR-HRS is required to provide mass-purified beams of exotic nuclides from the SPIRAL2 production building. A two-stage magnetic dipole mass separator has been designed for 60-keV beams up to mass number 300 (rigidity of 0.61 T-m). The mass dispersion allows a maximal resolving power $m/\Delta m$ of 31000 for a 1π-mm-mrad beam emittance. The small emittance is achieved using a buffer-gas-filled, linear quadrupole ion guide in front of the separator.

Introduction

The DESIR (Désintégration, Excitation et Stockage d'Ions Radioactifs) facility is part of the new equipment necessary for exploitation of the radioactive beams produced by SPIRAL2. DESIR includes a laboratory equipped with beam lines for low-energy experiments that can receive nuclides from the SPIRAL1, SPIRAL2 and S3 installations at GANIL. DESIR also includes an important instrument for beam purification, located in the production building of SPIRAL2: a high-resolution mass separator (HRS) for high-intensity beams (see Figure 1).

The DESIR-HRS includes two dispersive magnetic dipoles, preceded by a beam-cooling device [SHIRAC] that provides low-emittance beams for higher mass separation. Resolving power depends on magnetic dispersion and inversely on beam emittance. The concept of reducing the beam emittance for mass separation, originally conceived for the ISOLDE facility [ISOLDE] was elaborated in the context of the EURISOL Design Study [EURISOL].
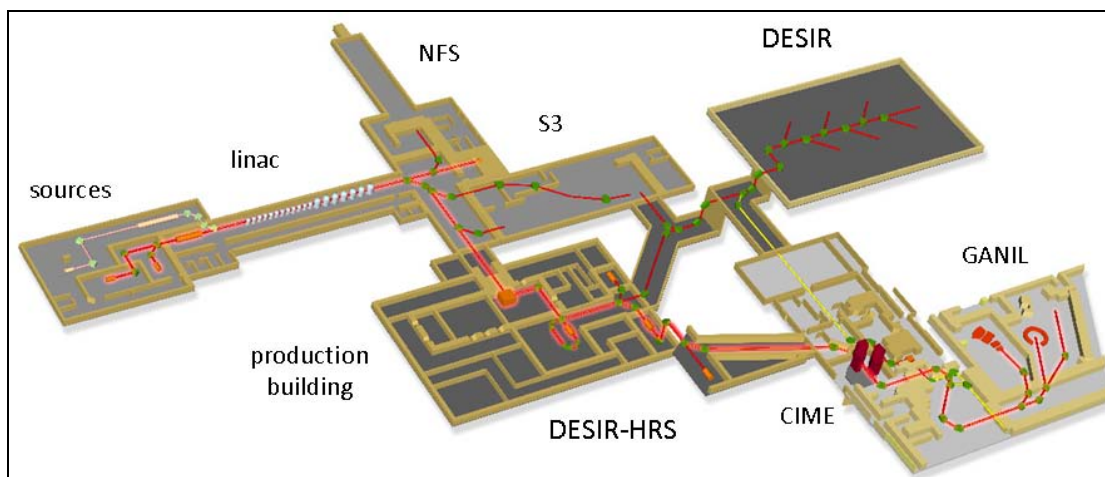

Figure 1: *Schematic layout of the entire GANIL facility including SPIRAL1, SPIRAL2, and DESIR.*

The beam cooler will provide the small emittance needed for the DESIR-HRS to achieve its design goal of a resolving power of $m/\Delta m = 20000$. As shown in Figure 2, a resolving power of 1000-2000 is enough to separate light exotic nuclei. However, for the medium-mass nuclei produced by SPIRAL2, a resolution well in excess of 10000 is needed.
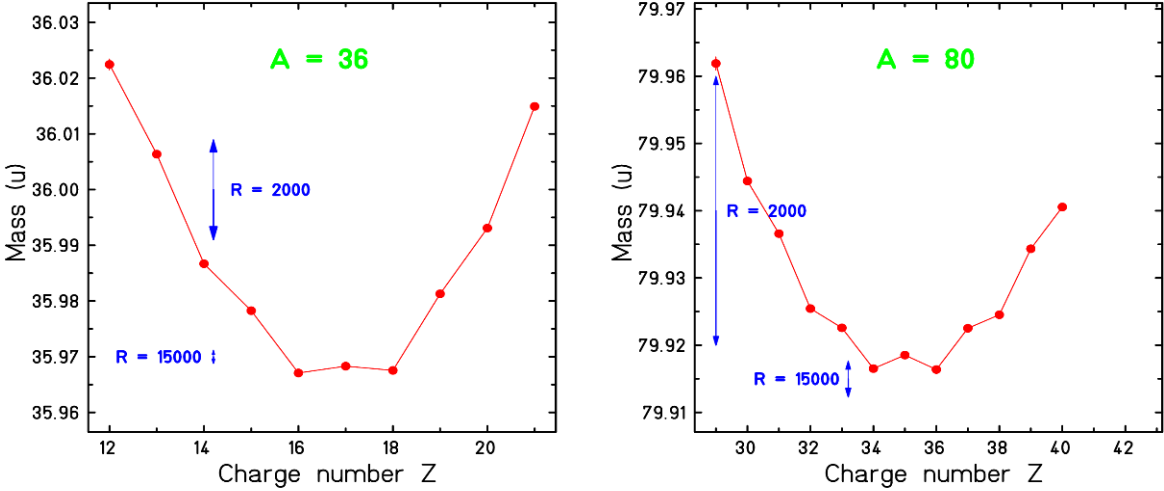

Figure 2: *Isobaric masses of A=36 (left) and A=80 (right) nuclides. The arrows indicate different mass resolving powers.*

SPIRAL2 is not the first radioactive beam installation to attempt the construction of an HRS. In fact, there is little success in obtaining high resolving power with magnetic dipoles, despite extensive efforts. The ISAC facility at TRIUMF recovered the mass separator from Chalk River Laboratories when the TASCC facility there was closed. At Chalk River, the separator achieved a resolving power of 20 000 using collimated (0.1 mm) stable beams and 5 700 for exotic species [CRNL]. ISAC typically operates with a lower resolving power, for ease of operation. The other example is the ISOLDE HRS, originally designed for 30 000, which routinely achieves only 4 500, although a different configuration is now used [ISOLDE]. The more recently designed separator for the CARIBU project [DAV08] has not yet achieved its design goal of 20 000, but tests are underway. A workshop was held at the CENBG (Bordeaux) where mass separator experts were able to discuss different approaches and the most plausible solution was unanimously a symmetric, two-stage solution.

The proposed design (see Fig. 3) consists of two 90-degree magnetic dipoles (D) with 36-degree entrance and exit angles, matching quadrupoles (MQ), focusing sextupoles (FS), focusing quadrupoles (FQ), and one multipole (M) with the configuration QQSQDMDQSQQ. Mirror symmetry is imposed with respect to the mid-plane to minimize aberrations. Focusing and corrective elements are all electrostatic and thus settings are independent of mass. To inject the purified beam into the 1+ line of the production building, a transport section is placed at the exit of the HRS, consisting of two quadrupole doublets and two 45-degree electrostatic benders. The detailed calculations are discussed in the following sections.
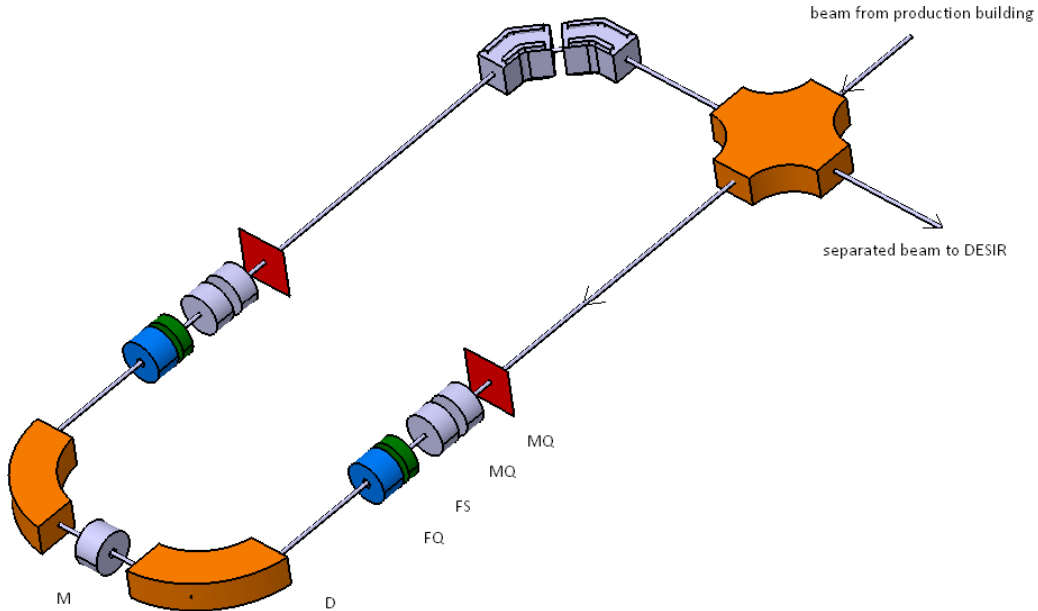
Figure 3: *Optical layout of the DESIR-HRS. Separation is performed using two 90-degree magnetic dipoles (D) with 36-degree entrance and exit angles. Mirror symmetry is imposed with respect to the mid-plane to minimize aberrations. The entrance beam optics was designed using matching quadrupoles (MQ), a focusing sextupole (FS), and a focusing quadrupole (FQ). A multipole (M) is placed at the mid-plane, between the two magnetic dipoles. The overall configuration is: MQ-MQ-FS-FQ-D-M-D-FQ-FS-MQ-MQ. After the second focal plane, two quadrupole doublets (not shown) and two electrical benders of 45° allow the system to match the 1+ line of SPIRAL2.*

DESIGN OF THE MAGNETIC DIPOLES

The magnetic dipoles are the most costly single elements of the DESIR-HRS. Simulations have been performed by the magnet group at GANIL using the following specifications:

Parameters for the Dipoles			
Characteristic	Value	Units	Comments
$B\rho_{max}$	0.45	Tesla-meters	
Vertical gap	0.07	meters	
Homogeneous region	0.40	meters	Transverse homogeneity optimized for 0.3 m, but still reasonable for 0.4 m
Curvature	0.85	meters	Beam bending radius
Angle	90	degrees	Beam bending angle
Pole face angles	36	degrees	Input and output

3

Simulations were made using the magneto-static module of the software OPERA. The dipoles have been designed in order to obtain the best homogeneity in the central zone, where most of the particles are transmitted. The field simulation and obtained homogeneity are shown in Fig. 4.
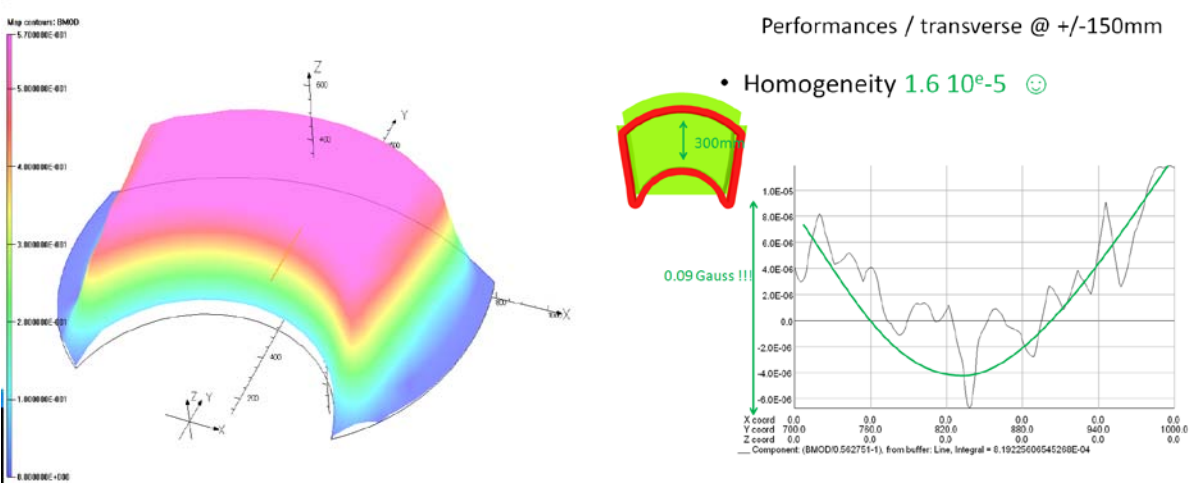

Figure 4: *Dipole field map and central homogeneity as calculated using TOSCA.*

The central (middle deviation) homogeneity obtained on the simulations represents the best we could achieve with the specifications, but it might be difficult to obtain over whole range of $B\rho$. At $B\rho_{min}$, the homogeneity is around 1.1×10^{-4}. The sensitivity of the homogeneity to several dimensions of the magnet has been evaluated with simulations to allow for deviations due to fabrication. The simulation field maps have been used in several beam optics calculations, in order to validate the design.

Design characteristics of the dipole			
Characteristic	Value	Units	Comments
Iron mass	6000	kg	Chosen to reduce saturation and variation of magnetic length
Copper mass	390	kg	
cooling circuits	6		per dipole
Cooling circuit length	74	m	per circuit
Conductor	8/8/4.5	mm	Width/height/hole diameter for the main power supply
Turns	96		
Current	210	A	maximum
Power supply	17	kW	not including correction coils

Note that this design is adapted to the $B\rho_{max}$, and is not suitable for higher magnetic rigidity, but the coil can be shared with a design adapted to $B\rho_{max} = 0.6$ T-m.

4

The geometrical characteristics of the dipole chosen to obtain good transversal homogeneity are shown in Fig. 5. The detailed mechanical design of the magnets can be seen in the figures. The full specifications will be described in the tender document that will be sent to prospective manufacturers.
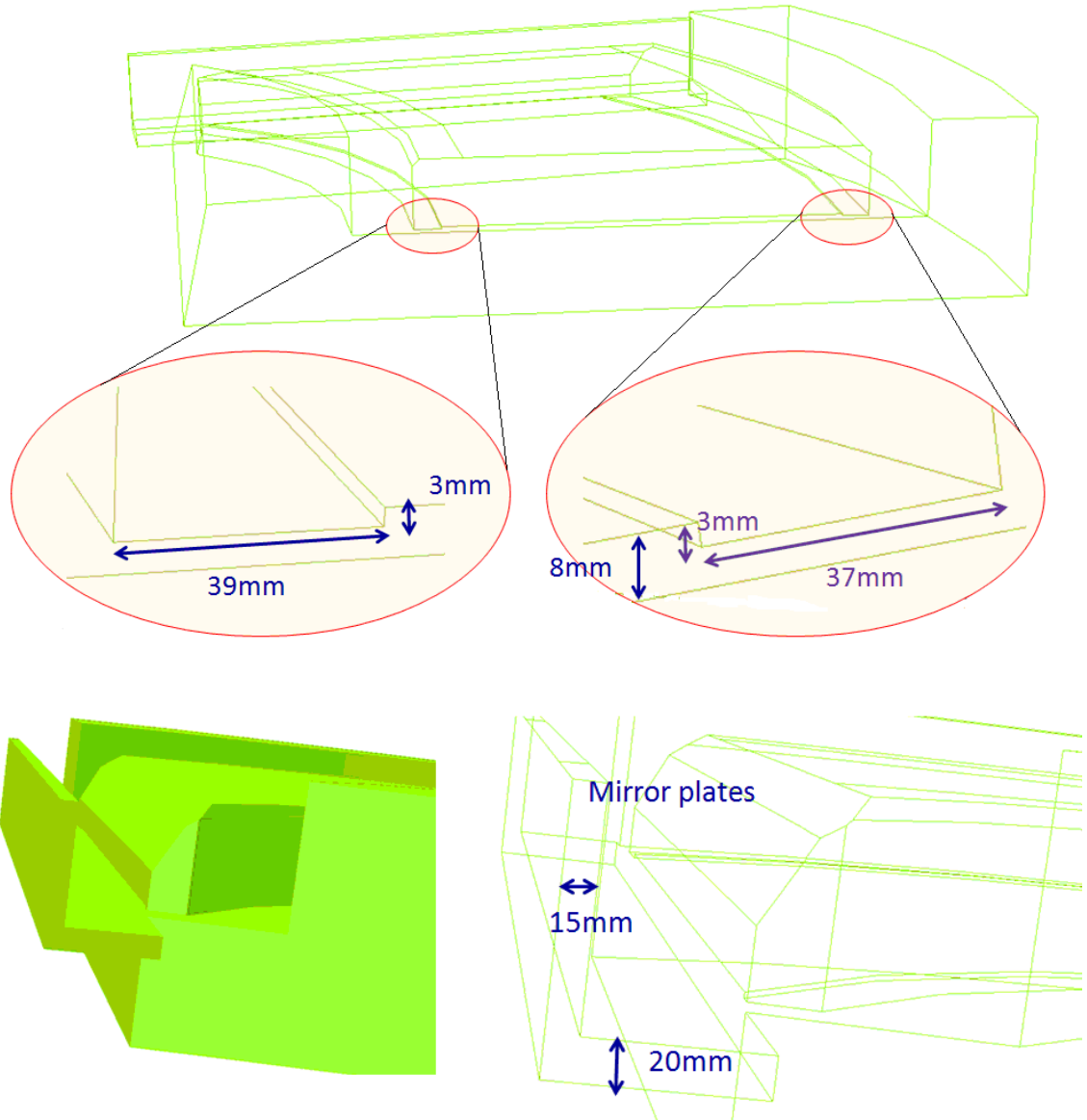

Figure 5: *Details of the dipole magnet geometry, including dimensions. This is just to show that the design of the magnets has reached an advanced stage. The full description of the geometry will be given in the tender document sent to prospective manufacturers. (top) the shim coil guide details and (bottom) the details for the fringe field end shielding.*

ION OPTICS, TRANSFER MATRIX AND BEAM ENVELOPES

The ion-optical code COSY INFINITY [Ber90] was used as a base of calculations. The phase space dimensionality used was 2, being the *x-a* (horizontal) as well as *y-b* (vertical) motion computed. δm is calculated as a parameter. Thus all calculations are performed in the following scaled coordinates:

$$[1] = x; [2] = a = p_x/p_0; [3] = y; [4] = b = p_y/p_0; [5] = \delta m = (m-m_0)/m_0$$

The beam enters the HRS by a 1 mm^2 slit, with a maximal angular dispersion of ±10 mrad and passes through the first quadrupole doublet, which consists of a pair of quadrupoles of opposite polarity. This matching section produces a ribbon-shaped beam. The next quadrupole makes the beam to diverge in radial (x-direction) and to converge in vertical. The divergent beam envelope is designed to occupy the entire dipole magnet acceptance to maximize mass dispersion. The combined effect of the entrance and exit angles of the dipoles produces a parallel beam in the radial direction. The focusing condition at the mid-plane is $(a,a) = (y,b) = (b,y) = 0$: point-to-parallel in x, and point-to-point/parallel-to-parallel in y. The symmetric half of the separator allows refocussing the beam to a 1 mm^2 envelope and making the mass selection with the slits placed at the image focal plane.

After the HRS, an ensemble of two quadrupole doublets and two 45° electrical benders allow to transport the beam until the compensation point of the 1+ line, homothetically (meaning: *different emittance but with the same relative orientation of the components*) at 80 π-mm-mrad. At this point the beam is considered as emitted from a minimum envelope of marginal dimensions of ± 2.25 mm horizontally and ± 7.45 mm vertically. The first order transfer matrix of at the image focal plane is:

	x_f	a_f	y_f	b_f						
$\frac{\partial}{\partial x_0}$	-1.000	-3.650	0.000	0.000		-	-	-	-	
$\frac{\partial}{\partial a_0}$	-0.397E-05	-1.000	0.000	0.000	$\frac{\partial}{\partial b_0}$	0.000	0.000	-0.601E-06	1.000028
$\frac{\partial}{\partial y_0}$	0.000	0.000	1.000	0.5013E-04	$\frac{\partial}{\partial \delta m}$	-31.32	-57.16	0.000	0.000

The calculated beam line envelopes are shown in the following figures. The following table summarizes the calculated parameters for the electrostatic elements.

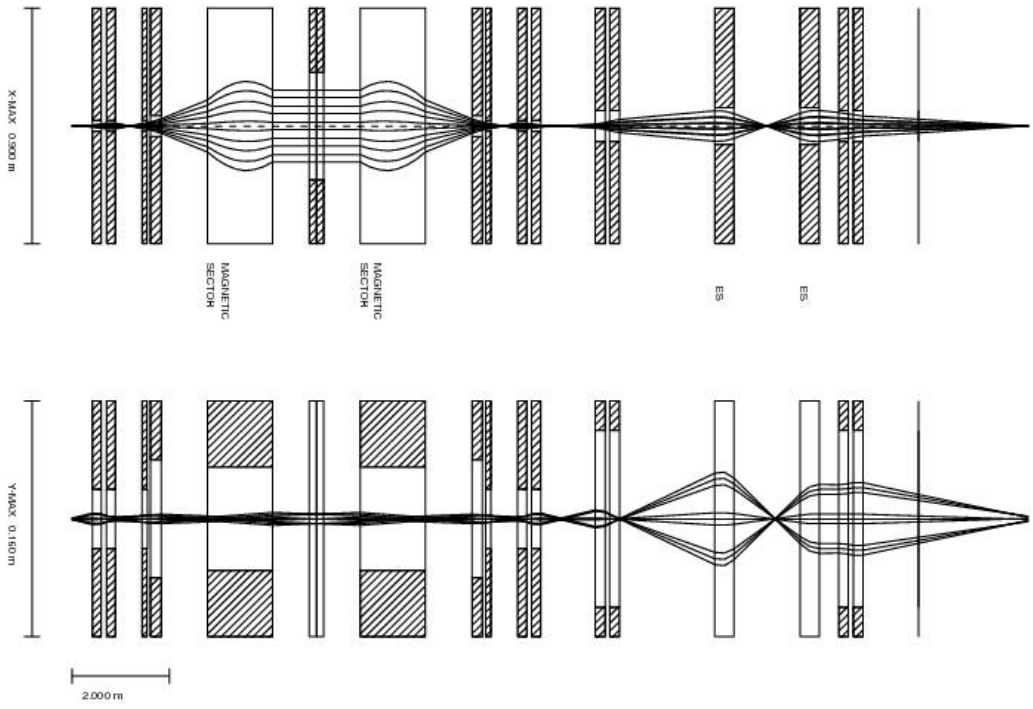| Parameters of electrostatic elements			
Element	Value (kV)	Element	Value (kV)
MQ1	-6.7E-01	M- Decapole	-1.8E-02
MQ2	7.6E-01	M- Dodecapole	-8.4E-03
FQ1	-8.6E-01	FQ3	-5.275
FS1	7.0E-02	FQ4	1.873
M- Sextupole	-7.6E-01	FQ5	0.361
M- Octupole	-6.0E-02	FQ6	-0.650

Figure 6: *Beam envelopes of the HRS in the x-(dispersive) and y-(non dispersive) planes calculated with the program* GICOSY [GICO]. *Please note the difference in the scale of both planes. The transport section for matching the 1+ line is included.*
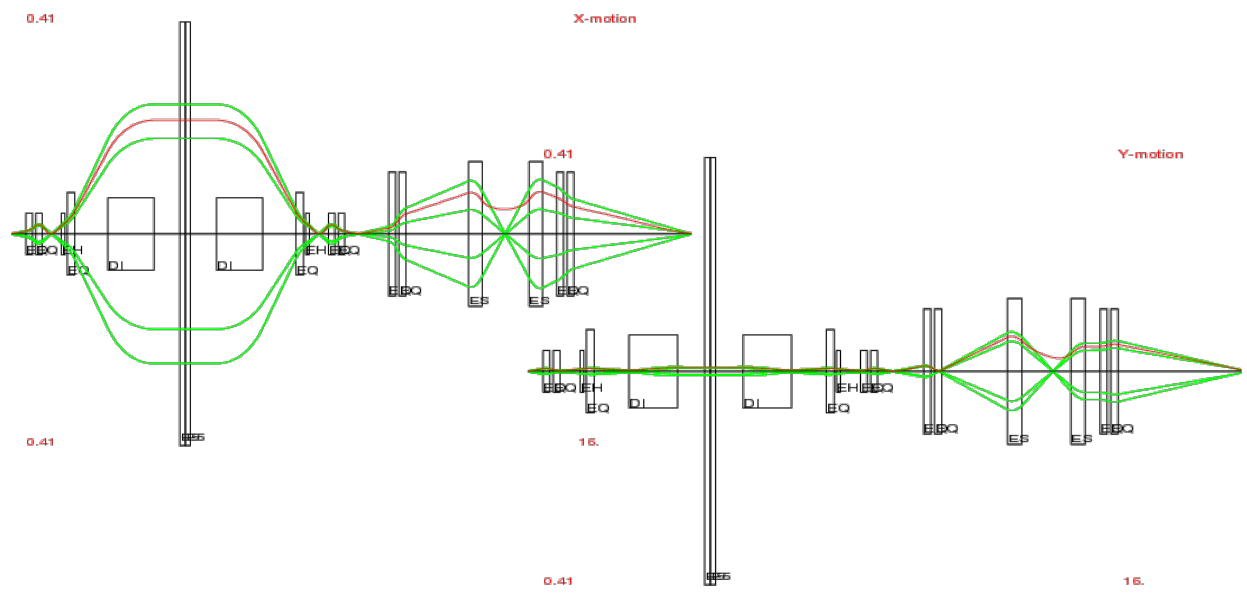

Figure 7: *Beam envelopes of the HRS in the x-(dispersive) and y-(non dispersive) planes calculated with COSY INFINITY.*

FIFTH-ORDER MONTE CARLO SIMULATION

In order to study the performance of the DESIR-HRS a Monte Carlo code has been developed. This code takes as input the transfer matrices as calculated from COSY INFINITY up to 5th order and propagates the beam through the different lattice elements. The output of the code are the initial and final phase spaces of the beam and the mass spectrum as calculated for the different masses introduced in the simulation. Fig. 8 shows the phase space diagrams after the separator assuming perfect geometrical alignment and the focal plane mass spectrum.
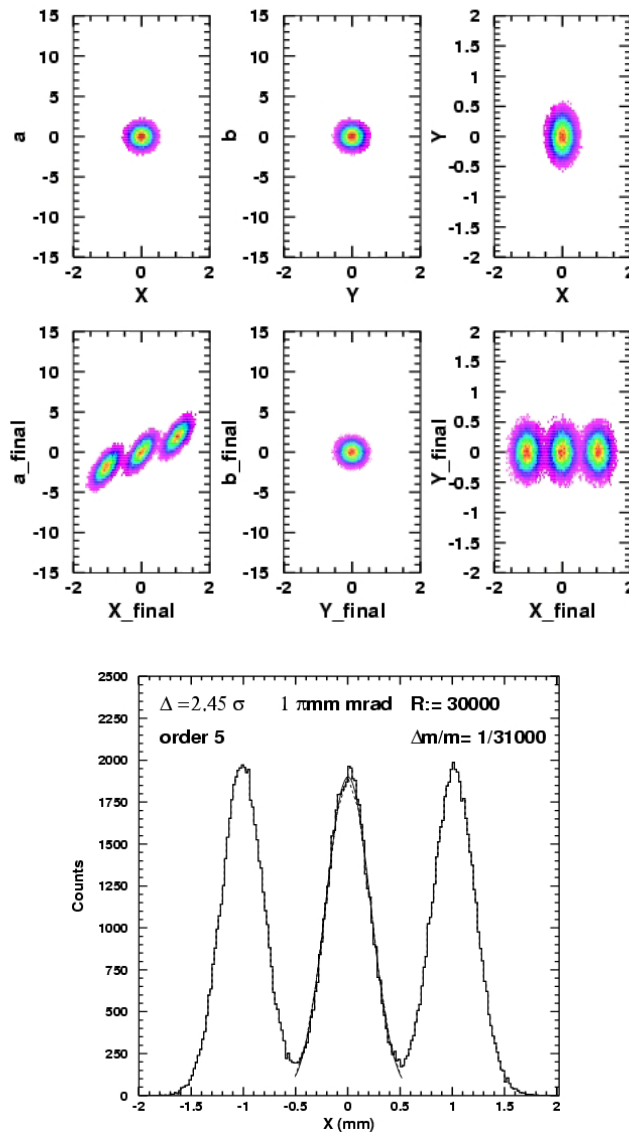

Figure 8: *Phase space calculated at 5th order for 50000 particules with mass deviations of -1/31000, 0, +1/31000. Top: Beam phase spaces at the exit of SHIRaC. Bottom: Phase spaces at the image focal point of the HRS. Mass spectrum calculated to 5th order for 50000 particules with mass deviations of -1/31000, 0, +1/31000.*

8

In order to simulate more realistic conditions reflecting manufacturing defects and optical element mis-alignment, the simulations were redone by varying the beam positions for each element according the to following table:

Module	ΔX(mm)	ΔY(mm)	$\Delta \theta$(°)
1	+0.1	-0.1	-0.2
2	-0.1	+0.1	+0.2
3	-0.05	-0.05	-0.2
4	+0.1	+0.1	+0.2
5	-0.1	-0.1	-0.2
X-Offset (mm)	-0.09		
R	20477		

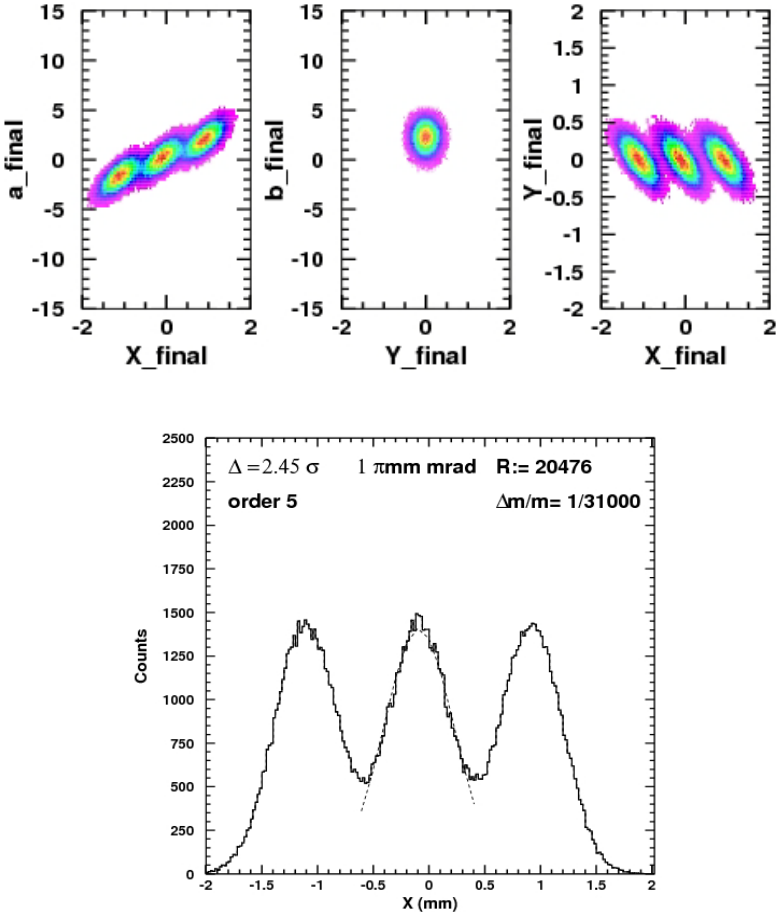The corresponding phase space plots and mass spectrum are showing in Fig. 9.

Figure 9: *Top: Phase space after the separator calculated using the maximal tolerance on the misalignment of the different optics modules, calculated at 5th order for 50000 particules with mass deviations of -1/31000, 0, +1/31000. Bottom: corresponding mass spectrum, showing the mass resolution decreased to ~20000.*

The above simulations assume that the neighboring isobaric masses are of equal intensity, which is rarely the case in reality. Another simulation was performed to take this into account. The following table lists isobaric beam intensities that are predicted by production simulations within the SPIRAL2 project.

Element	I (pps) [SPIRAL2]	$\Delta m/m$ [Ame2003]	Δx (mm)
Cd	$3.5\,10^2$	$-2.1\,10^{-4}$	$+6.5$
In	$1\,10^6$	$-1.2\,10^{-4}$	3.6
Sn	$9.5\,10^8$	0	0
Sb	$1.9\,10^9$	$+2.5\,10^{-5}$	-0.8
Te	$6.6\,10^9$	$+7.0\,10^{-5}$	-2.2
Xe	$7.4\,10^{10}$	$+1.0\,10^{-4}$	-3.2
Ba	$2.2\,10^1$	$+9.7\,10^{-5}$	-3.1

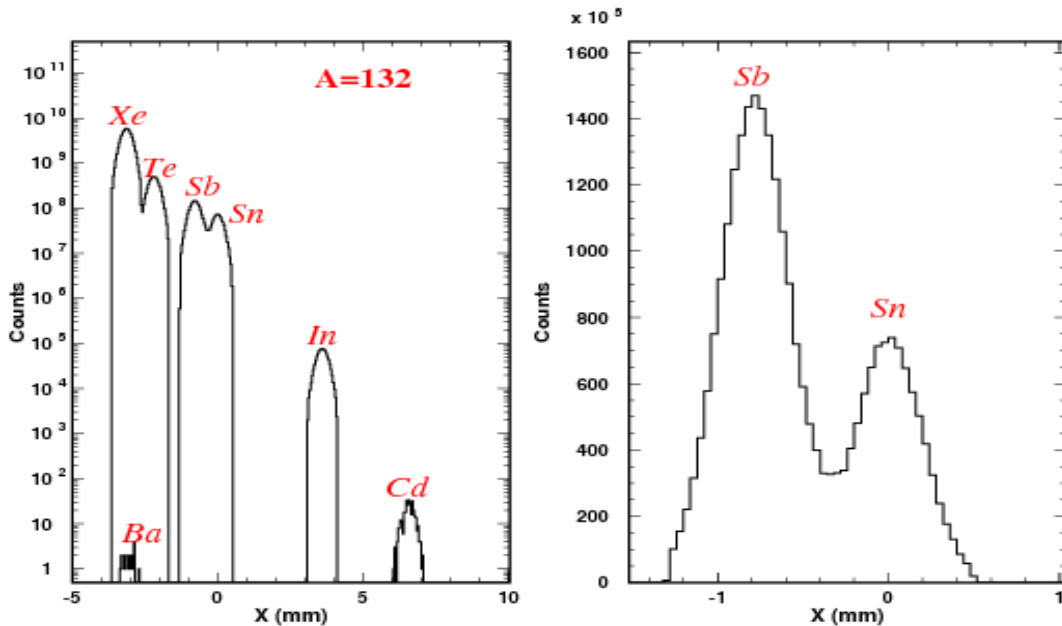The resulting mass distributions are shown in Fig. 10.

Figure 10: *Left: Mass spectrum calculated at 5th order considering all A=132 elements produced from n-induced fission 50-kW deuteron beam, a 280-g (3.5-g/cm^3) UCx target, with the separator tuned to center ^{132}Sn. Intensities are taken from [SPIRAL2]. Right: Zoom of the mass spectrum in linear scale. The colored zone indicates slits which, if placed at ± 0.5mm, the transmission of ^{132}Sn is 97% with a 13.3% contamination of ^{132}Sb. If the slits are closed to ±0.25 mm the contamination is eliminated but the transmission of ^{132}Sn is reduced to 61%.*

MODULE INTEGRATION

For safety requirements of the SPIRAL2 project, the DESIR-HRS is divided into seven modules, each of which is separated by gate valves, as shown in Figure 11. Each module can be isolated and removed independently in case of contamination. The seven modules essentially follow the DESIR-HRS optics design: (1) injection quad-quad and hex-quad lenses; (2) first magnetic dipole; (3) electrostatic multipole; (4) second magnetic dipole; (5) extraction quad-quad and hex-quad lenses; (6) first 45-degree bender; (7) second 45-degree bender.
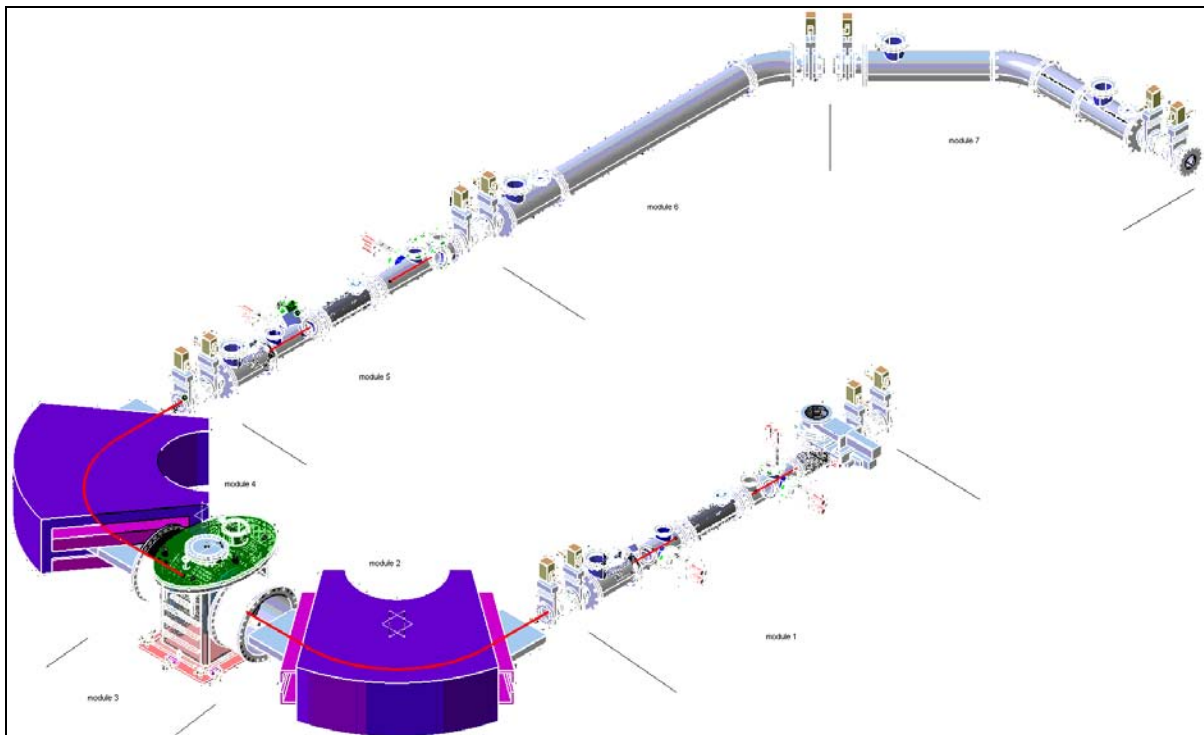

Figure 11: *Modular structure of the DESIR-HRS required by the SPIRAL2 safety authorities.*

Summary and outlook:

The design for the DESIR High Resolution Separator (DESIR-HRS) is now essentially complete. The design takes into account past experience from separator experts at radioactive beam installations worldwide. Several ion optics codes have been used to verify coherence of the optical solutions and to cross check the predicted performance. The different codes

include: COSY INFINITY, TRANSPORT, GALOP, ZGOUBY and GICOSY, with calculations up to 5th order.

The design of the HRS relies on a strong optical focussing for a wide illumination of small dipoles in order to minimize the size of the separator. This optical condition makes the system more sensitive to the fringe field effects and to the homogeneity of the dipole field. A correct simulation of such effects is important in order to predict the necessary corrections. Simulations using TOSCA and SIMION8 show that this will be feasible. The design for the magnetic dipoles also includes the possibility of easily changing magnetic edges to refine the minimization of aberrations.

Considering the maximal tolerance on the misalignment of the different modules as verified with the land surveyor of the project, a resolution of ~20 000 can be achieved for a beam emittance of 1 π-mm-mrad at 60 keV.

References

[DAV08] C. Davids, D. Peterson, Nucl. Instr. Meth. Phys. Res. B **266** (2008) 4449 (2008).

[Ber90] M. Berz, Nucl. Instr. and Meth. A **298** (1990) 473

[EURISOL] Beam Preparation (chapter 6) in: The EURISOL Design Study Final Report, J. Cornell (ed.) GANIL press, 2009

[GICO] Program GICOSY, http://www-linux.gsi.de/~weick/gicosy/

[TRAN] PSI Graphic Transport Framework by U. Rohrer based on a CERN-SLAC-FERMILAB version by K.L. Brown et al.

[TURT] PSI Graphic Transport Framework by U. Rohrer based on a CERN-SLAC-FERMILAB version by K.L. Brown et al.

[CRNL] K.S. Sharma et al., Nuclear Instruments and Methods in Physics Research A275 (1989) 123-132; and H. Schmeing et al., Nuclear Instruments and Methods 186 (1981) 47-59

[ISOLDE] T.J. Giles et al., Nuclear Instruments and Methods in Physics Research B 204 (2003) 497–501

[SHIRAC] O. Gianfrancesco et al., Nuclear Instruments and Methods in Physics Research B 266 (2008) 4483-4487; F. Duval, Ph.D. thesis, U. Basse Normandie (2010)

[SPIRAL2] http://pro.ganil-spiral2.eu/spiral2/spiral2-beams/radioactive-ion-beams-of-spiral2/low-energy-desir-isol-rib-beams-available-for-the-day-1-spiral2-phase-2-experiments/intensities-from-n-induced-fission

[AME2003] G. Audi, A.H. Wapstra, C. Thibault, Nuclear Physics A 729 (2003) 337

APPENDIX 1: LATTICE CONFIGURATION FOR THE HRS

Module HRS			
Element	**Distance (mm)**	**Element**	**Distance (mm)**
Drift length L1 (diagnostics)	420	Drift length L6	750
Matching quadrupole MQ1 aperture = 40 mm	185	Dipole D2 ρ = 850 mm, θ = 90º $\beta1=\beta2=36º$ Pole gap = 70 mm, width = 400 mm	1335
Drift length L2	100	Drift length D1 (Slits)	955
Matching quadrupole MQ2 aperture = 40 mm	185	Focus quadrupole FQ2 aperture = 80 mm	220
Drift length L3 (slits)	275	Drift length L5	60
Drift length L4 (diagnostics)	275	Focus sextupole FS2	110
Focus sextupole FS1	110	Drift length L4 (Diagnostics)	275
Drift length L5	60	Drift length L3 (Slits)	275
Focus quadrupole FQ1 aperture = 80 mm	220	Matching quadrupole MQ3 aperture = 40 mm	185
Drift length D1 (Slits)	955	Drift length L2	100
Dipole D1 ρ = 850 mm, θ = 90º $\beta1=\beta2=36º$ Pole gap = 70 mm, width = 400 mm	1335	Matching quadrupole MQ4 aperture = 40 mm	185
Drift length L6	750	Drift length L1	420
Multipole M aperture = 410 mm,	300	Slits	

Beam Transport to the 1+ Line			
Element	**Distance (mm)**	**Element**	**Distance (mm)**
Drift length L7	850	EB ρ = 500 mm, θ = 45º, a = 140 mm	392.70
Quadrupole FQ3, a = 120 mm	200	Drift length L11	400
Drift length L8	100	Quadrupole FQ5 a = 120 mm	200
Quadrupole FQ4 a = 120 mm	200	Drift length L12	100
Drift length L9	1807.93	Quadrupole FQ6 a = 120 mm	200
EB ρ = 500 mm, θ = 45º, a = 140 mm	392.70	Drift length L12	1142.93
Drift length L10	1353.5	1+ Line Dipole	

Appendix 2: Performance study of the HRS using the code *Raytracing Turtle*

A set of simulations has also been performed for the DESIR-HRS by using the program *Raytracing Turtle* [TURT]. These versions were calculated and optimised using TRANSPORT [TRAN] to third order. Three isobars differing in mass by ±1/20000 were simulated. The transmission and the contamination to the central mass by the neighbourgs were calculated. All calculations were perfomed using a momentum dispersion of $\Delta p/p = \pm 0.0005$. The beam had 1mm width both in x- and y-directions. Two values for θ_{max} and φ_{max} were studied: ±2 and ±10 mrad, corresponding to the respective beam emittances: 1 π-mm-mrad and 5π-mm-mrad.

Figure 12 shows the spatial separation at the image focal point, for three isobars differning in mass by ±1/20000 for a beam emittance of 1π mm.mrad. Placing slits XY of 1mm^2, the transmision is of 86%. The cross-contamination is ~0%
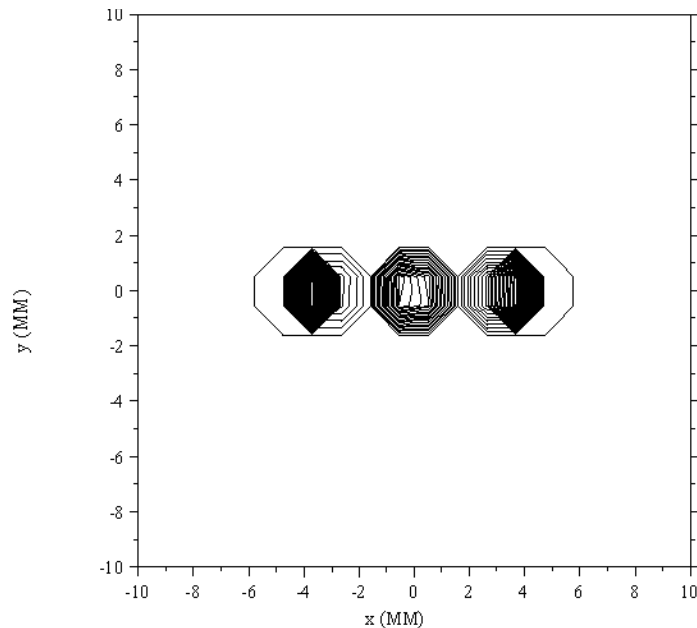

Figure 12: *Performance of the HRS as calculated with TURTLE for 1π mm.mrad, Δp/p=0.0005 and Δm/m=20000.*

For a beam emittance of 5π mm.mrad, we obtain a transmission of 45% at the focal point of the HRS and a cross-contamination of 1.5%.